JOURNAL OF MATERIALS SCIENCE 30 (1995) 2733–2737

Processing-induced resistive barriers in ZnO varistor material

D. C. HALLS
Department of Materials, Imperial College of Science, Technology and Medicine, London SW7 2BP, UK

C. LEACH
Manchester Materials Science Centre, University of Manchester and UMIST, Manchester M1 7HS, UK

Evidence is presented for the origin of high-resistivity barriers at certain interfaces in high-field varistor materials. The barriers give rise to terrace contrast which can be observed using remote electron beam induced current imaging in the SEM. It is proposed that these interfaces, which are often associated with a thick intergranular layer of a compositionally distinct bismuth rich oxide, are relicts of the powder structure and correspond to agglomerate surfaces. It is suggested that the presence of these resistive surfaces ultimately limits the current that can flow at breakdown.

1. Introduction

Zinc oxide varistors are described as "passively smart" materials and are used in the electronics industry for the suppression of high-voltage transients. They show markedly non-linear electrical properties having very high resistances at low voltages but very low resistances at high voltages [1] enabling appropriate circuitry to shunt away voltage spikes from sensitive equipment. The non-linear resistive behaviour mimics the breakdown observed in back-to-back zener diodes but with greater energy-handling capabilities [2].

Varistors are conveniently classified into two types: high-field varistors and low-field varistors [3]. Low-field varistors are mass produced and have grain sizes between 10 and 30 μm, whereas high-field varistors of the type described in this contribution have much smaller grain sizes, typically a few micrometres or less, and are manufactured for specific applications which are mainly military in nature [4]. In general, they are more compact than the low-field variety, breaking down at higher internal field gradients.

The varistor's microstructure consists of grains of n-type semiconducting zinc oxide surrounded or partially surrounded by an intergranular phase. This intergranular material contains other metal oxide additives and can vary in thickness and composition [5]. Gupta [6] has classified these oxides into three groups. There are varistor formers, such as bismuth, antimony, barium and praseodymium, that induce the varistor action, performance enhancers such as cobalt, manganese, nickel and chromium which improve the non-linearity of the I–V curve and improve the energy-absorption capabilities of the material, and performance highlighters, including additives such as sodium, aluminium, potassium and gallium that are capable of stabilizing the non-linear function. Additions of PbO and Bi_2O_3 are also used to promote densification during hot pressing [3]. CoO has been shown to give enhanced varistor performance when the powder is milled directly with ZnO and then calcined, causing the cobalt ions to diffuse into the ZnO grains to give zincite [3, 7] before the addition of the lead and bismuth oxides. Kim *et al.* [8] have suggested that cobalt forms states 1.2 eV above the ZnO valence band, increasing the electron-hole generation rate and thus helping the tunnelling breakdown mechanism. Additionally, these additives may also affect grain-growth rates and thus affect the breakdown voltages attainable, for a given size of material.

During the preparation of ceramic powders, steps that include precipitation from solution give rise to accumulations of new material on the surfaces of flocced or agglomerated particles suspended in the solution. Under changing conditions of precipitation, the developing agglomerate's surface chemistry is likely to be different from that of the bulk. Likewise, diffusion processes occurring during the calcination of powders can result in compositional differences between the bulk of the agglomerates and their surfaces as well as the partial sintering of the interior of the agglomerates. It is therefore the case that the structure of the agglomerates produced during the calcination step can affect the distribution of the oxides that are introduced later, particularly if those so formed are hard or impermeable.

Charge collection mode imaging has been used in the SEM to investigate the electrical properties of, primarily, semiconducting materials. The particular imaging mode used here has previously been termed

0022–2461

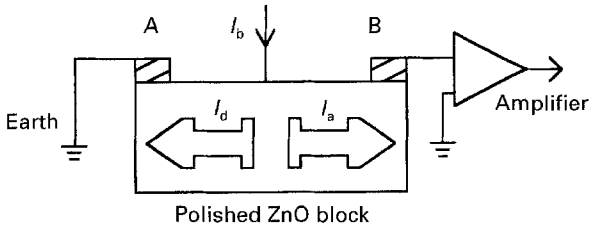

Figure 1 Sample geometry used for REBIC imaging in the SEM. The absorbed component of the beam current, I_b, can flow to earth either directly through electrode A or indirectly via the amplifier through electrode B.

remote electron beam induced current (REBIC) in semiconductor research [9].

The sample geometry used for REBIC imaging in the SEM is shown in Fig. 1. When the electron beam, I_b, strikes the sample surface between the two electrodes, the resistive components of the specimen act as a current divider. Part of the absorbed current flows to earth through electrode A and the remainder is collected at electrode B and amplified to form the image.

If the beam current is considered to be constant, then the total absorbed specimen current at any point on the sample surface will be modulated by variations in the emitted current (principally secondary and backscattered electron currents). For an electrically homogeneous material of fixed composition the current passing through electrode B to the amplifier should vary linearly with distance from that electrode and a uniform gradation of contrast should be observed in the image. In real materials, other contrast effects are superimposed on this model. For example, there may be contrast due to variations in the emitted current, current amplifications due to charge separation effects may be observed (termed electron beam induced current or EBIC) or local differences in the rate of change of contrast may be seen due to local resistivity variations. Whilst true EBIC is only rarely observed in ZnO [10], resistivity variations are believed to give rise to the step or "terrace" contrast observed by numerous workers [11, 12].

This paper describes the relationship between agglomerates in the varistor powder prior to sintering and the distribution of resistive barriers in the fired ceramic by comparing observations of the powder structure in green and partly sintered compacts with conductive mode imaging in the SEM.

2. Experimental procedure

Raw varistor powders were prepared by a chemical precipitation route. An intimate mixture of zinc oxide and cobalt oxide was produced by calcination of precursors prior to the addition of other oxides such as bismuth oxide, lead oxide and aluminium oxide in solution. The solutions were then spray dried and calcined at 600 °C.

Small amounts of powder and partially sintered pellets were examined to study the microstructural evolution of the powder agglomerates present in the powder.

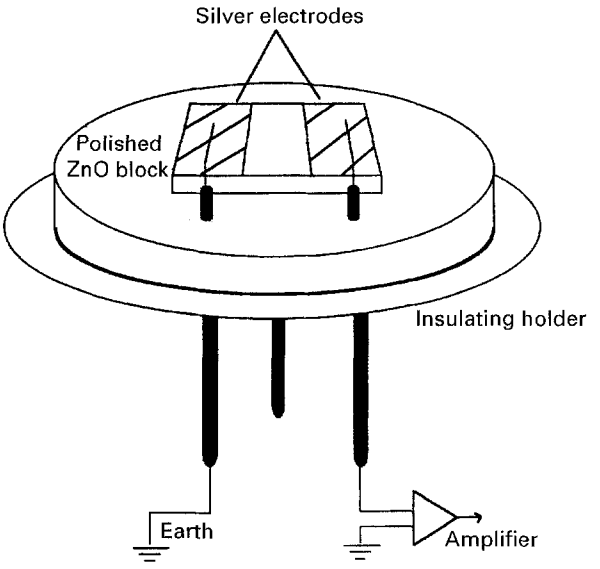

Figure 2 Schematic drawing of the sample as prepared for REBIC examination in the SEM.

Blocks, 5 mm × 5 mm square, of fully sintered ZnO varistor material were cut using a diamond saw. These were then ground flat and polished on nylon cloth using a water-based slurry of 0.3 μm α-alumina powder. A pair of parallel silver electrodes was painted on to the polished surfaces of the material to which electrical contacts were made (Fig. 2). The exposed polished area between the electrodes was then examined using the charge collection mode of the scanning electron microscope. For all experiments a Jeol JSM840A fitted with a Matelect ISM-5 EBIC amplifier and a Kontron image analyser were used.

3. Results

3.1. Powder structure

Fig. 3a shows the powder structure as comprising spherical agglomerates. The diameters of the larger agglomerates are in the range 10–20 μm.

Fracture surfaces of pellets, partially sintered to densities of 65% and 80%, are seen in Fig. 3b and c, respectively. The powder agglomerate structures are still clearly visible in the materials after partial sintering.

3.2. Microscopy

Fig. 4a shows a low-magnification secondary electron image of the sintered varistor. The electrodes used for REBIC imaging are clearly visible at the left and right edges of the image. Fig. 4b shows a REBIC image of the same area as Fig. 4a. The steps in contrast giving rise to a terrace effect are clearly visible. No equivalent contrast is observed in the secondary electron image.

Fig. 4c is a higher magnification secondary electron image of the sample in which the grain size can be seen to be in the range 2–5 μm. Fig. 4d is the corresponding backscattered electron image (compositional) in which the bismuth phases can be seen as bright patches on some zinc oxide grain boundaries. The REBIC image

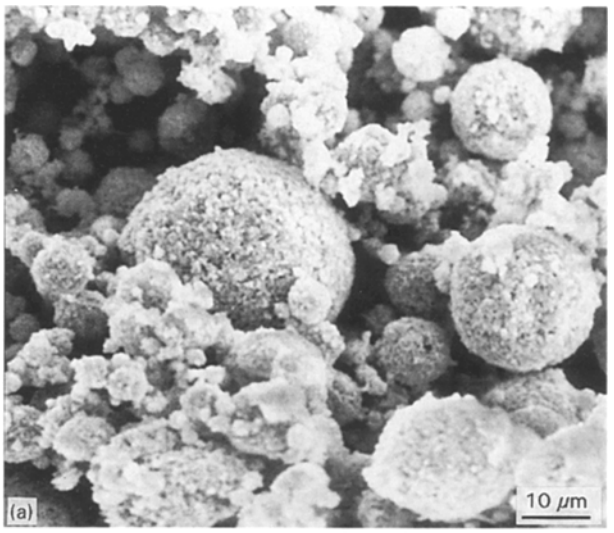

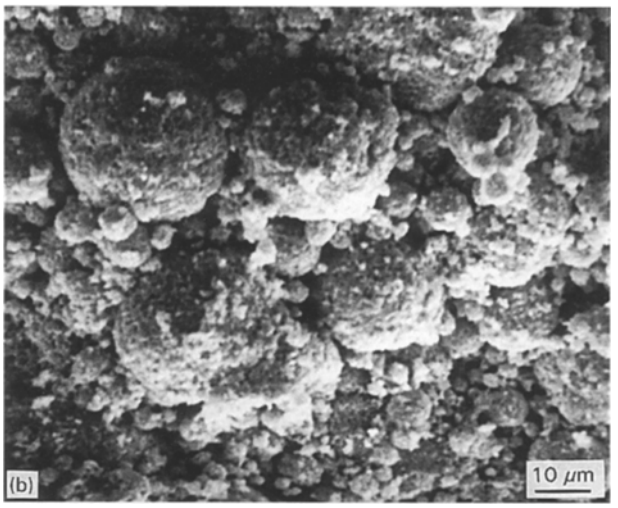

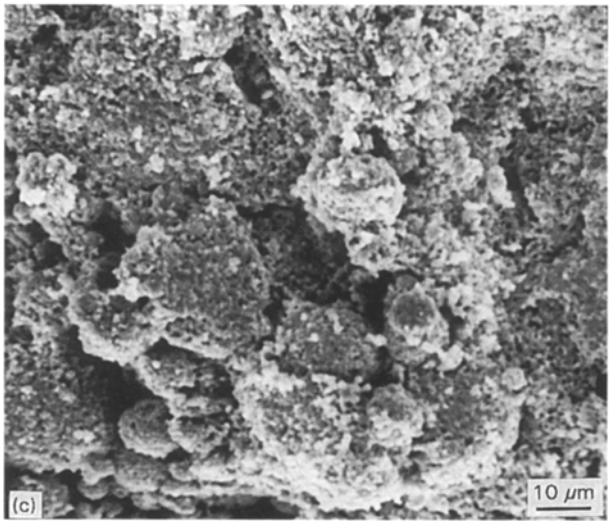

Figure 3 SEM secondary electron images of (a) the powder, and of fracture surfaces of pellets sintered to (b) 65% and (c) 80% density.

of the same area, shown in Fig. 4e, clearly shows the presence of step contrast. The resistive barriers giving rise to this effect do not occur at every grain boundary but are separated by approximately 20–30 μm.

An alternative method of imaging the step contrast boundaries is shown in Fig. 4f. Here one of the sample electrode contacts is made with a point contact (micromanipulator probe) inside a region bounded entirely by high-resistivity interfaces. Other similarly bounded regions are observed and their dimensions correspond well with the size of the larger agglomerates estimated from the powder micrographs.

4. Discussion

It is well known that agglomerate size and structure affects the compressibility and hence the compaction properties of the ceramic powder [13]. Additionally, there is a tendency for agglomerates to densify much more rapidly internally during the sintering process than with neighbouring material [14]. Thus certain agglomerate structures can lead to heterogeneous densification effects on sintering with residual porosity at agglomerate interfaces. The observation of relict agglomerate textures in our partially sintered materials demonstrates that is indeed the case here.

The enhanced porosity at agglomerate boundaries in the partly sintered material may affect the process of liquid-phase sintering brought about by the action of the bismuth oxide phases [15]. This would occur by allowing the bismuth to flow into the porous regions around the zinc oxide agglomerates forming regions of bismuth-rich second-phase material. Conductive mode imaging has shown these structures to be highly resistive giving rise to the observed step contrast. In addition lines of porosity associated with the incomplete densification of inter agglomerate boundaries appear to increase the resistivity of the material locally, leading to similar steps in contrast.

Fig. 4f shows the dimensions of the structures bounded by high-resistance interfaces to be in the same range as the agglomerate sizes. When the sample is imaged in REBIC mode between parallel electrodes the structures align and we see banding in this material similar to that reported by other workers [11, 12]. The plateaux between the terraces are between two and five grains wide and it is suggested that the plateaux formed from intra-agglomerate densification with the terraces defining the inter-agglomerate boundaries which acted as barriers to grain growth due to their relatively poor densification.

The electrical behaviour of these resistive interfaces and their contribution to the overall properties of the varistor are not understood at the moment, and is the subject of current activity. Certainly the resistance of the terrace boundaries is greater than that within the terraces, but it is unclear whether both types of grain boundary show the varistor effect. Ineffective grain boundaries have been described in the literature [16, 17] and ascribed both to oxygen deficiency and the presence of second phases. The compositional differences associated with powder agglomeration and the presence of open pore networks during densification would suggest that the two types of grain boundary considered here have the opportunity to show variations in either of these qualities.

Conductive mode analysis of commercial mass-produced low-field varistors (work in hand) show

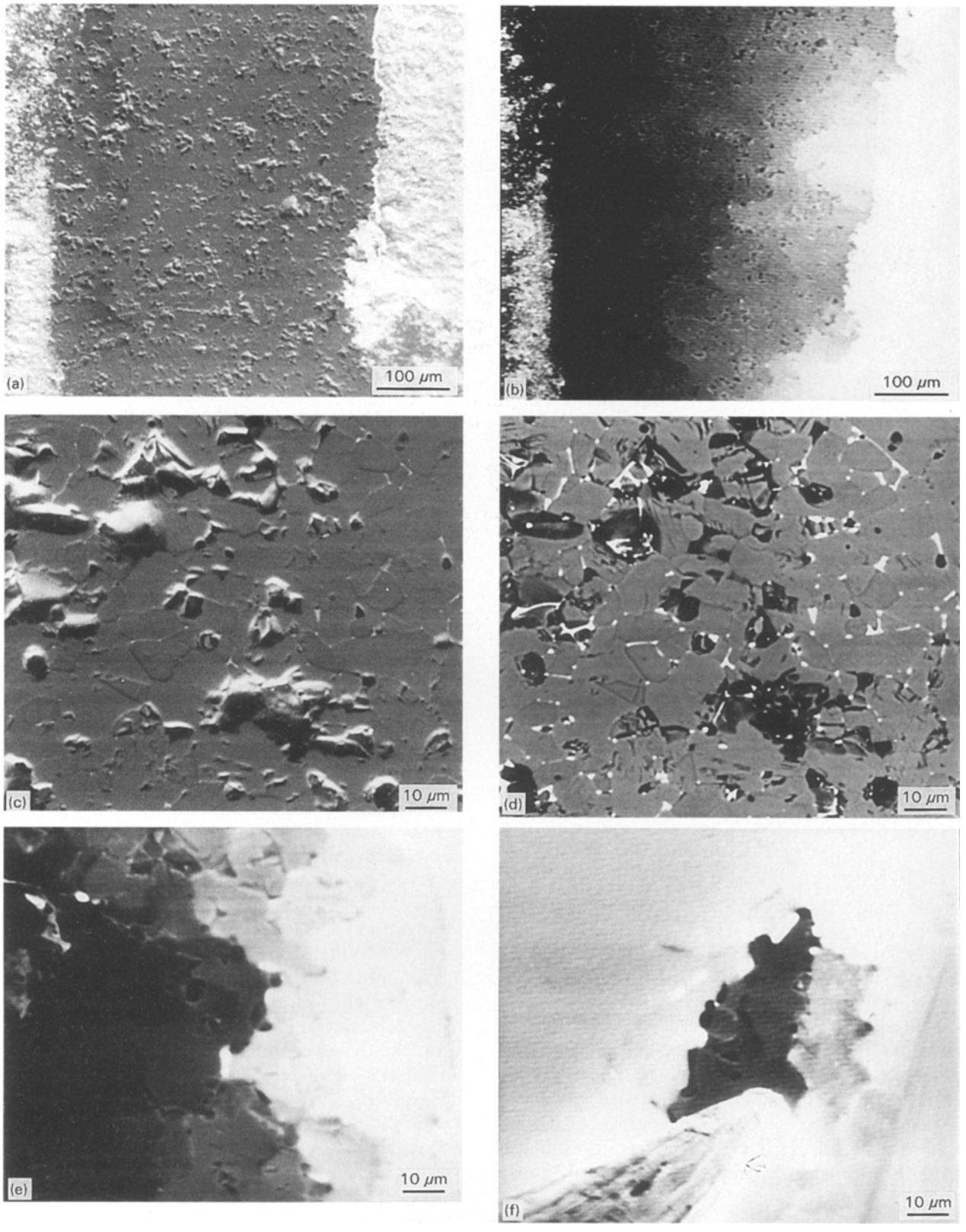

Figure 4(a, b). Low magnification secondary electron and REBIC images, respectively, of ZnO. (c–e) Corresponding higher magnification secondary, backscattered and REBIC images, respectively, of ZnO. (f) A REBIC image taken using a slightly different current collection geometry.

clearly defined step-contrast effects similar to those described here. It may be that these resistive interfaces, generated as a relic of powder agglomerate interfaces, may ultimately limit the maximum current which can pass through the varistor during breakdown.

Additional insulating phases have been identified by other workers to occur heterogeneously at grain boundaries in varisting materials. In low-field varistors, common insulating phases are spinel ($Zn_7Sb_2O_{12}$) and pyrochlore ($Zn_2Sb_3Bi_3O_{14}$) [18] which are detrimental to varistor action, although they have a positive effect in limiting grain growth. Previous work on high-field materials has shown the phases $ZnCo_2O_4$ and Co_3O_4 to be present [3, 7].

Olsson and Dunlop [17] have demonstrated that many interfaces in low-field varistors containing the pyrochlore phase do not show the varistor effect. It was also demonstrated by characterizing individual grain boundaries that many interfaces have larger or smaller breakdown values than the mean value. Schwing and Hoffmann [19] also demonstrated a higher than normal breakdown voltage of approximately 6 V on a bicrystal interface containing a continuous film of oxide additives 5 μm in thickness.

5. Conclusion

The results strongly suggest that the formation of electrical step contrast is due in this case to the effects of agglomerate structures in the original powder. These create resistive barriers which may ultimately limit the amount of current able to pass through the device at breakdown. By using a processing procedure that addresses the problem of agglomeration during precipitation it may be possible to obtain higher overall breakdown current values.

References

1. M. MATSUOKA, *Jpn J. Appl. Phys.* **10** (1971) 736.
2. L. M. LEVINSON and H. R. PHILLIP, *Ceram. Bull.* **65** (1986) 639.
3. G. S. SNOW, S. SPENCER WHITE, R. A. COOPER and ARMIJO RUDY, *J. Ceram. Bull.* **59** (1980) 617.
4. H. R. PHILLIP and L. M. LEVINSON, *J. Appl. Phys.* **52** (1981) 1083.
5. L. M. LEVINSON and H. R. PHILLIP, *ibid.* **46** (1975) 1332.
6. T. K. GUPTA, *J. Mater. Res.* **7** (1992) 3280.
7. R. J. LAUF and W. D. BOND, *Ceram. Bull.* **63** (1984) 278.
8. S. K. KIM, H. H. OH and C. K. KIM, *Jpn. J. Appl. Phys.* **30**(B) (1991) 1917.
9. L. O. BUBALEK and W. E. TENNENT, *Appl. Phys. Lett.* **52** (1988) 1255.
10. J. D. RUSSELL, D. HALLS and C. LEACH, *J. Mater. Sci. Lett.*, in press.
11. A. BERNDS, K. LOEHNERT and E. KUBALEK, *J. Phys. Coll.* **C2** (1984) 861.
12. D. B. HOLT, *Solid State Phenom.* **37–38** (1994) 171.
13. A. AL-TOUNSI, R. PUYANE and M. S. J. HASHMI, *J. Mater. Proc. Technol.* **37** (1993) 543.
14. A. J. MOULSON and J. M. HERBERT, in "Electroceramics, Materials, properties, applications" (Chapman and Hall, London, 1990).
15. R. EINZINGER, *Appl. Surf. Sci.* **1** (1978) 329.
16. ZE-CHUN CAO, RU-JUN WU and RUN-SHENG SONG, *Mater. Sci. Eng.* **B22** (1994) 261.
17. E. OLSSON and G. L. DUNLOP, *J. Appl. Phys.* **66** (1989) 3666.
18. E. OLSSON, G. DUNLOP and R. OSTERLUND, *J. Am. Ceram. Soc.* **76** (1993) 65.
19. U. SCHWING and B. HOFFMANN, *J. Appl. Phys.* **57** (1985) 5372.

Received 28 October 1994
and accepted 9 January 1995